Enhanced spin-current tensor contribution in collision dynamics

Yoritaka Iwata[1] and Joachim A. Maruhn[2]
[1]*GSI Helmholtzzentrum für Schwerionenforschung, D-64291 Darmstadt, Germany*
[2]*Institut für Theoretische Physik, Universität Frankfurt, D-60325 Frankfurt, Germany*
(Received 15 December 2010; revised manuscript received 26 April 2011; published 28 July 2011)

The tensor and spin-orbit forces contribute essentially to the formation of the spin mean field, and give rise to the same dynamical effect, namely spin polarization. In this paper, based on time-dependent density functional calculations, we show that the tensor force, which usually acts like a small correction to the spin-orbit force, becomes more important in heavy-ion reactions and the effect increases with the mass of the system.

DOI: 10.1103/PhysRevC.84.014616 PACS number(s): 25.70.Jj, 21.60.Jz, 21.30.Fe

I. INTRODUCTION

The tensor force, which is necessary to explain the properties of the deuteron, has attracted special attention recently, because it has turned out to play an essential role in the existence limit of exotic nuclei, as well as the nuclear shell structure far from the β-stability line (for example, see [1–8]). An important feature is that the spatial average of the tensor operator is exactly equal to zero (for example, see [9]). On the other hand, the spin-orbit force, which is necessary to explain the large spin polarizations of scattered nucleons, plays a crucial role in the nuclear shell structure. The origin of the tensor force can be found in the one-pion exchange potential, and that of the spin-orbit force in the relativistic aspects of quantum dynamics.

Thus the tensor and spin-orbit forces are quite different in their origins, while resulting in the same dynamical effect, namely, spin polarization. Spin polarization, which arises mostly from the spin-orbit force, spontaneously takes place in the early stage of heavy-ion reactions, and affects the equilibration process to a large extent. Concerning microscopic time-dependent Skyrme energy density functional (Skyrme-EDF) calculations, the appearance of spontaneous spin polarization even in central collisions between β-stable nuclei was shown, and its origin was clarified to be the time-odd part of the spin-orbit force [10]. Therefore, the enhancement or reduction of spin polarization gives an ideal framework to pin down the properties of the tensor force in collision situations.

In this paper, the role of the tensor force in heavy-ion reactions is investigated based on time-dependent density functional calculations with explicitly implemented spin current tensor terms in Skyrme-EDF. Special attention is paid to the effect of such contributions on time evolution. As a result, some information on the importance of the contribution from the tensor force in heavy-ion reactions is presented.

II. THEORETICAL FRAMEWORK

A. Mean field due to spin-orbit and spin-current tensor contributions

The contribution of the tensor force, whose role was underestimated and mostly neglected for a long time, was substantially studied in the context of Skyrme-EDF only recently [5–8]. Here much attention is paid to clarify the role of the tensor force in spin polarization.

Let us begin with the corresponding functional form in the Skyrme-EDF. Let ρ, $\mathbf{s}$, and $\mathbf{J}$ denote the number density, spin density, and spin-orbit density, respectively. The spin-orbit field has the form

$$\mathbf{W}_q(\mathbf{r}) \cdot (-i)(\nabla \times \boldsymbol{\sigma}), \tag{1}$$

where $\boldsymbol{\sigma}$ denotes the Pauli matrices, and $q = n, p$ (n and p stand for neutron and proton, respectively). $\mathbf{W}_q(\mathbf{r})$, is decomposed into the spin-orbit and spin-current tensor contributions:

$$\mathbf{W}_q(\mathbf{r}) = \mathbf{W}_q^{LS}(\mathbf{r}) + \mathbf{W}_q^{T}(\mathbf{r}), \tag{2}$$

where $\mathbf{W}_q^{LS}(\mathbf{r})$ and $\mathbf{W}_q^{T}(\mathbf{r})$ denote the form factors of spin-orbit and spin-current tensor mean fields, respectively. The contribution of the spin-orbit force [11] is represented by

$$W_q^{LS}(\mathbf{r}) = \tfrac{1}{2} W_0[\nabla\rho(\mathbf{r}) + \nabla\rho_q(\mathbf{r})],$$

where $\rho = \rho_p + \rho_n$, and W_0 is a constant. Among the many possible terms, we deal only with the vector part of the spin-current pseudotensor density (namely, $\mathbf{J}^2$ term). That contribution is represented by

$$\mathbf{W}_q^{T}(\mathbf{r}) = \alpha \mathbf{J}_q(\mathbf{r}) + \beta \mathbf{J}_{q'}(\mathbf{r}) \tag{3}$$

with $q' = n, p$ satisfying $q \neq q'$, according to Stancu-Brink-Flocard [12]. This consists of the contribution from the tensor force and the exchange part of the central force, and it is impossible to disentangle both components, since only the sum is fitted; here is the reason why we are interested not only in the effect of pure tensor force but also in the effect arising from Eq. (3). Note that even the central force part of the tensor terms [a part of the first term of the right-hand side of Eq. (3)], whose contribution in collision situations was discussed in [13], was not taken into account for some modern Skyrme parametrizations such as SLy4 [14], SLy4d [15], and SKM* [16], while included in SLy5 [14]. Indeed, this term makes the global fitting process more difficult (e.g., see [17,18]).

Although the full introduction of the tensor force requires more terms compared to those shown in Eq. (3) (see [6] for the full expression, and [19,20] for the parameter-dependent complicated results), we restrict ourselves to the contribution arising from Eq. (3) in order to evaluate its effects on the

spin polarization and the dissipation dynamics. Indeed, the contribution arising from Eq. (3) corresponds to a direct modification of the spin-orbit contribution. In the following we refer to $\mathbf{W}_q^T(\mathbf{r})$ of Eq. (3) simply as "spin-current tensor terms," although they correspond, strictly speaking, only to a part of these terms.

The introduction of $\mathbf{W}_q^T(\mathbf{r})$ alone breaks the Galilean invariance, so that a spurious excitation might appear [10,21]. Note that there is no symmetry breaking, if all the terms that arise from tensor force are taken into account. This point is discussed by comparing exactly the same calculations in two different reference frames: the center-of-mass frame and the laboratory frame, which should show the importance of such spurious excitations.

B. Spin-current tensor contribution in collision situations

A framework for measuring the effects of the tensor force is presented with a focus on collision dynamics. Concerning the spin polarization, it is reasonable to begin with a discussion of spin-orbit coupling. It is defined by the scalar triple product

$$\mathbf{L}\cdot\mathbf{S} = (\mathbf{r}\times\mathbf{p})\cdot\mathbf{S} = (\mathbf{p}\times\mathbf{S})\cdot\mathbf{r}, \tag{4}$$

where $\mathbf{L}$ and $\mathbf{S}$ denote angular momentum and spin angular momentum, respectively. In collision situations $\mathbf{r}\times\mathbf{p}$ is related to the impact parameter. Comparing Eqs. (1) and (4), $\mathbf{W}_q(\mathbf{r})$ in Eq. (1) plays the role of the vector $\mathbf{r}$ in Eq. (4), where the momentum $\mathbf{p}$ is replaced approximately by ∇ in the Skyrme-EDF.

In order to evaluate the spin-current tensor contribution to spontaneous spin polarization, we introduce a proper theoretical setting of heavy-ion collisions. Our starting point is that the tensor and the spin-orbit forces are difficult to compare in collision dynamics, if there is no similarity in their spatial patterns. Let the reaction plane be (x, z) with the initial collision direction z, and the direction perpendicular to the reaction plane be y. For simplicity, the spin direction of the initial state is assumed to be parallel to the y axis. In this setting, because only the z component of $\mathbf{p}$ and the y component of $\mathbf{S}$ are nonzero, we have

$$\mathbf{L}\cdot\mathbf{S} = \left(p_y S_z - p_z S_y\right) x = -p_z S_y x. \tag{5}$$

We see that only the x component of the vector $\mathbf{r}$, and thus the x component of $\mathbf{W}_q(\mathbf{r})$ play a role. In this setting, the role of the spin-current tensor terms in the spin polarization can be evaluated by the corresponding x component of $\mathbf{W}_q^T(\mathbf{r})$. Accordingly, the spin-current tensor and spin-orbit contributions can be compared, if there is a certain similarity between the x components of $\mathbf{W}_q^T(\mathbf{r})$ and $\mathbf{W}_q^{LS}(\mathbf{r})$ (otherwise attraction or repulsion happen irregularly from place to place). Note that their similarity, which will be shown to be true, is not trivial. In the following the x components of $\mathbf{W}_q^T(\mathbf{r})$ and $\mathbf{W}_q^{LS}(\mathbf{r})$ are simply represented by $W_q^T(\mathbf{r})$ and $W_q^{LS}(\mathbf{r})$, if there is no ambiguity.

III. DYNAMICAL SPIN-CURRENT TENSOR EFFECT

A. Spontaneous spin polarization

A systematic three-dimensional time-dependent density functional calculation is carried out in a spatial box $48\times48\times48$ fm^3 with a spatial grid spacing of 0.8 fm. The relative velocity in the collisions is set to 10% of the speed of light, and the initial distance of the colliding nuclei to 20.0 fm; their initial positions are (0,0,10) and (0,0,−10). In order to pay attention to the mass-dependent general features, we consider central collisions between identical $N = Z$ nuclei: ^{16}O + ^{16}O, ^{40}Ca + ^{40}Ca, and ^{56}Ni + ^{56}Ni. Some features of the tensor force acting on $N = Z$ bound nuclei were studied in [8]. The contributions from $\mathbf{J}_q$ and $\mathbf{J}_{q'}$ in Eq. (3) are not so different for collisions between $N = Z$ nuclei, therefore the force parameter dependence mostly arises from the sum of α and β. To understand the dependence of spin polarization on the sum of parameters $\alpha+\beta$, we employ systematic SV-tls parameter sets [22], in which $\alpha+\beta$ values vary from positive to negative (Table I). The SV-tls parameter sets were lately introduced in the context of refitting the spin-current tensor contribution including only the central force part. The obtained systematic result is utilized to interpret the contribution from the spin-current tensor terms fitted including the tensor force. Indeed, the two force parameter sets labeled SLy5+T and Stancu have the opposite sign for the value of $\alpha+\beta$ (for more examples of $\alpha+\beta$ values of the other parameter sets, see [6]). Note again that once the values of α and β are fixed, we cannot distinguish the two origins of the spin-current tensor contribution, i.e., whether it is derived from the tensor force or the central force.

Let us begin with obtaining a rough estimate on the amplitude due to the spin-orbit tensor contribution, where

TABLE I. Force parameter sets in use: systematic SV-tls parameter sets [22], SLy5+T [7], a tensor force parameter set added to SLy5 parameter set, and Stancu [12,23], a tensor force parameter set added to SkM* and SLy4d parameter sets. In particular, SV-tls ($\eta_{\rm tls} = k$) are parameter sets fitted by fixing the value $\eta_{\rm tls}$ in [22] to be equal to k; $\eta_{\rm tls} = 1$, 0, and −1 correspond to the cases with the spin-current tensor terms (simply denoted by SV-tls, if there is no ambiguity), those without spin-current tensor terms (SV-bas in [22]), and those with the anti-spin-current tensor terms, respectively. Note that because α and β also appear in the remainder of the spin-current tensor terms, the refit process does not necessarily require that α and β for SV-tls ($\eta_{\rm tls} = 1.0$) be equal to $-\alpha$ and $-\beta$ for SV-tls ($\eta_{\rm tls} = 1.0$).

Parameter set	SV-tls ($\eta_{\rm tls} = 1.0$)	SV-tls ($\eta_{\rm tls} = 0.4$)	SV-tls ($\eta_{\rm tls} = -0.4$)	SV-tls ($\eta_{\rm tls} = -1.0$)	SLy5+T	Stancu
α [MeV fm^{-5}]	71.102	34.981	−21.714	−51.940	−89.8	154.39
β [MeV fm^{-5}]	35.141	27.427	−1.488	1.714	51.1	139.91
$\alpha+\beta$ [MeV fm^{-5}]	106.243	62.408	−23.202	−50.226	−38.7	294.30

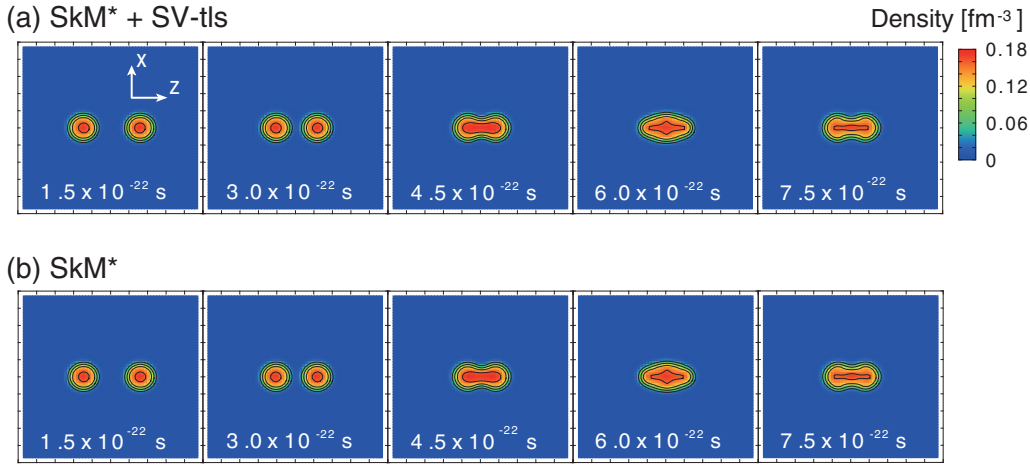

FIG. 1. (Color online) Time evolution of ^{40}Ca + ^{40}Ca at the bombarding energy 130 MeV (c.m.). Snapshots of the density are shown in a fixed square (40 × 40 fm^2) on the reaction plane, where contour lines are plotted for multiples of 0.04 fm^{-3}. Time evolutions shown in (a) and (b) correspond to the cases with or without the spin-current tensor terms, respectively. For (a), the parameter set SV-tls is used for the spin-current tensor part, and SkM* for the remainder.

the Skyrme-force parameter set SV-tls [22] is taken for the spin-current tensor part, and SkM* for the remainder including the spin-orbit force. Figure 1 shows the time evolution of ^{40}Ca + ^{40}Ca resulting in fusion, where the cases with or without the spin-current tensor terms are compared with respect to the density. Omitting the spin-current tensor contribution while including the spin-orbit contribution shows no notable difference to the density evolution with all force terms included. On the other hand, the same calculation without the spin-orbit contribution does not achieve fusion. This suggests that large dissipation arises from the spin-orbit force, while the spin-current tensor contribution is definitely small. Similar results are obtained for cases when the force parameter SkM* is replaced by SLy4d.

For the spin-polarization, we consider the y projection of spin for each single nucleon. The spin distribution of the colliding nuclei is calculated by their superposition:

$$s_y(t, \mathbf{r}) = \rho(t, \mathbf{r})_\uparrow - \rho(t, \mathbf{r})_\downarrow,$$

where $\rho(t, \mathbf{r})_\uparrow$ and $\rho(t, \mathbf{r})_\downarrow$ denote the densities of spin-up and spin-down components, respectively. The value of $s_y(t, \mathbf{r})$ is positive if the spin-up component is more abundant, zero for saturated spins, and negative otherwise. As is seen from the presence of S_y in Eq. (5), the problem of comparing the different role of spin-current tensor and the spin-orbit contributions becomes meaningless if spontaneous spin polarization is absent. Spin polarization appears for all the reactions and all the force parameter sets used (Table I); e.g., in Fig. 2, the presence of spin polarization is shown for ^{40}Ca + ^{40}Ca.

Figure 2 shows a typical example of spin polarization during heavy-ion collisions, where SV-tls parameter set is employed for both spin-current tensor and the reminder parts. Strong spin polarization is confirmed to be located on the edge of the density distribution. The spin distribution is point symmetric with respect to the origin, which reflects the symmetry of the central collision. Note that the spatial average of spin polarization for the spin-saturated system is equal to zero. As a result, the concept of examining the spin-current tensor contribution in the presence of spin polarization is valid and will be carried out in the following.

B. Enhancement

Comparison between the two different frames enables to evaluate the amplitude of spurious excitation caused from the introduction of $\mathbf{W}_q^T(\mathbf{r})$. The ratio of spurious excitation is summarized in Table II, where the expectation value for spurious excitation is estimated by the difference of values between the center-of-mass and laboratory frames. We see that the spurious excitation is quite small even limited to the spin-current tensor contributions. Such tendency is also valid for all the reactions and all the force parameter sets used; e.g.,

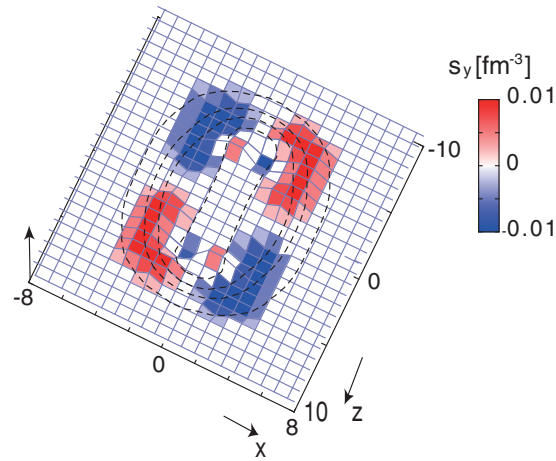

FIG. 2. (Color online) Spin distribution (the spin is projected onto the y axis) of a composite nucleus at $t = 6.0 \times 10^{-22}$ s is shown in a square (20 × 16 fm^2) on the reaction plane (SV-tls). For reference, contours of the density distribution are also shown (contour − 0.01, 0.06, 0.11, and 0.16 fm^{-3}).

TABLE II. Spurious excitation for ^{40}Ca + ^{40}Ca. The ratio of spurious excitation in the form factors is shown.

Parameter set	$\mathbf{W}_p^T(\mathbf{r})$[%]	$\mathbf{W}_p^{LS}(\mathbf{r})$[%]
SV-tls ($\eta_{\rm tls} = 1.0$)	0.29	0.003
SV-tls ($\eta_{\rm tls} = 0.4$)	0.13	0.043
SV-tls ($\eta_{\rm tls} = -0.4$)	0.67	0.018
SV-tls ($\eta_{\rm tls} = -1.0$)	0.74	0.042
SLy5+T	1.26	0.13
SkM*+Stancu	2.14	0.37
SLy4d+Stancu	2.45	0.14

spurious excitation ratios are 1.82% in $\mathbf{W}_p^T(\mathbf{r})$ and 0.11% in $\mathbf{W}_p^{LS}(\mathbf{r})$ for ^{16}O + ^{16}O [SV-tls ($\eta_{\rm tls} = 1.0$)], and 0.13% in $\mathbf{W}_p^T(\mathbf{r})$ and 0.012% in $\mathbf{W}_p^{LS}(\mathbf{r})$ for ^{56}Ni + ^{56}Ni [SV-tls ($\eta_{\rm tls} = 1.0$)].

We investigate the spin-current tensor contribution in a composite nucleus formed briefly after the full-overlap situation ($t = 6.0 \times 10^{-22}$ s). In case of ^{40}Ca + ^{40}Ca (SV-tls), Fig. 3 compares the x components of $\mathbf{W}_q(\mathbf{r})$ for the spin-current tensor and spin-orbit terms. Both distributions are antisymmetric with respect to the z axis, and have similar distributions but different signs and amplitudes. It is clearly seen that the spin-current tensor contribution is opposite to the spin-orbit contribution, and amounts to less than 10% of the latter. It follows that the total contribution from spin-current tensor and spin-orbit terms is not so different from the contribution of the spin-orbit terms alone. No significant difference is noticed between the values for protons and neutrons, which is expected for a collision between $N = Z$ nuclei. The smallness of the spin-current tensor contribution compared to the spin-orbit contribution is found to hold

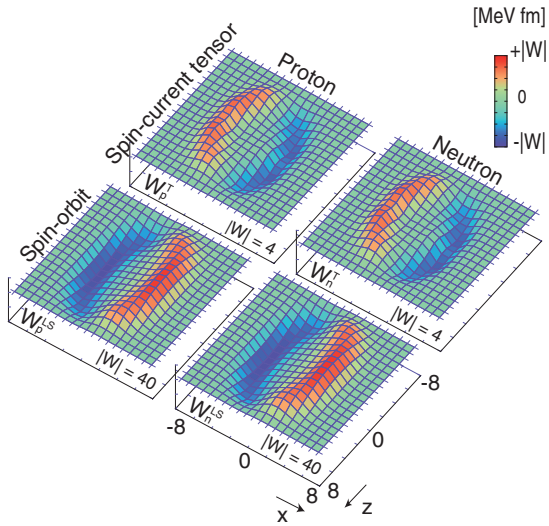

FIG. 3. (Color online) Snapshots of the x component of $\mathbf{W}_q(\mathbf{r})$ at $t = 6.0 \times 10^{-22}$ s projected on the reaction plane (SV-tls). The values are plotted in a square (16×16 fm^2) on the reaction plane separately for the spin-current tensor and spin-orbit contributions, and for protons ($q = p$) and neutrons ($q = n$), respectively. The maximum amplitude $|W|$ of the function is shown in the lower right-hand side of each plot.

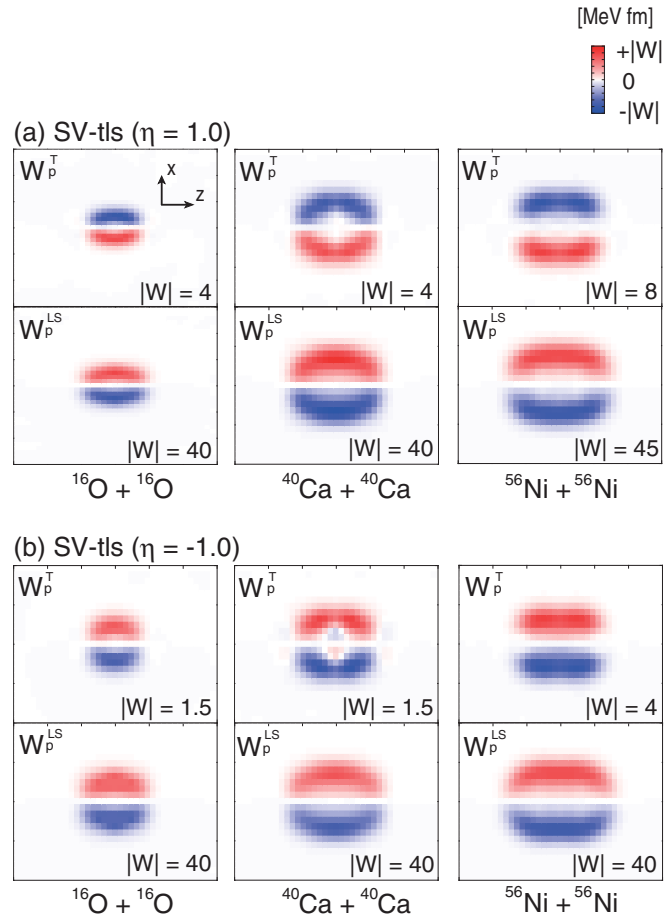

FIG. 4. (Color online) Snapshots of the x-components of the form factors of spin mean field $\mathbf{W}_p^T(\mathbf{r})$ (upper ones in each panel) and $\mathbf{W}_p^{LS}(\mathbf{r})$ (lower ones in each panel) at $t = 6.0 \times 10^{-22}$ s are shown in a square (30×20 fm^2) on the reaction plane. Calculations using SV-tls ($\eta_{\rm tls} = 1.0$) and SV-tls ($\eta_{\rm tls} = -1.0$) are shown in (a) and (b), respectively. The maximum amplitude $|W|$ of the function is shown in the lower right-hand side of each plot.

regardless of the choice of force parameter set and the mass of the colliding nuclei (Fig. 4 and Table III). In particular, for the force parameter dependence, the ratio between spin-current tensor and spin-orbit contributions

$$\mathbf{W}_q^T/\mathbf{W}_q^{LS}(t) = \frac{\sum_{\mathbf{r}} \left|\mathbf{W}_q^T(t,\mathbf{r})\right|}{\sum_{\mathbf{r}} \left|\mathbf{W}_q^{LS}(t,\mathbf{r})\right|} \tag{6}$$

at $t = 6 \times 10^{-22}$ s is summarized in Table III. On the contrary, the difference in sign depends on the force parameter set (compare the upper and the lower panels of Fig. 4). The signs between $\mathbf{W}_q^T(\mathbf{r})$ and $\mathbf{W}_q^{LS}(\mathbf{r})$ are opposite for SV-tls ($\eta_{\rm tls} = 1.0$), SV-tls ($\eta_{\rm tls} = 0.4$), SkM*+Stancu, and SLy4d+Stancu, but the same for SV-tls ($\eta_{\rm tls} = -1.0$), SV-tls ($\eta_{\rm tls} = -0.4$), and SLy5+T. This characteristic feature precisely coincides with the sign of $\alpha + \beta$. There is a notable increase with mass for the spin-current tensor contributions, while it is only modest for those of the spin-orbit contributions.

Let us move on to the time-dependent features of the spin-current tensor contribution. In case of ^{40}Ca + ^{40}Ca (SV-tls), the

TABLE III. Smallness of the spin-current tensor contribution for ^{40}Ca + ^{40}Ca. Ratio between spin-current tensor and spin-orbit terms [shown in Eq. (7)] is calculated for different force parameter sets and isospins. The expected uncertainties due to spurious excitation are shown as errors.

Parameter set	$\mathbf{W}_p^T(\mathbf{r})/\mathbf{W}_p^{LS}(\mathbf{r})$[%]	$\mathbf{W}_n^T(\mathbf{r})/\mathbf{W}_n^{LS}(\mathbf{r})$[%]
SV-tls ($\eta_{\rm tls} = 1.0$)	6.52 ± 0.04	6.56 ± 0.05
SV-tls ($\eta_{\rm tls} = 0.4$)	4.38 ± 0.02	4.37 ± 0.01
SV-tls ($\eta_{\rm tls} = -0.4$)	1.40 ± 0.02	1.44 ± 0.02
SV-tls ($\eta_{\rm tls} = -1.0$)	3.22 ± 0.05	3.33 ± 0.05
SLy5+T	21.99 ± 0.61	21.54 ± 0.62
SkM*+Stancu	13.87 ± 0.49	13.84 ± 0.44
SLy4d+Stancu	16.85 ± 0.55	16.81 ± 0.56

time evolution of Eq. (6) is shown in Fig. 5 for center-of-mass and laboratory frames. The corresponding x components of $\mathbf{W}_p^T(\mathbf{r})$ and $\mathbf{W}_p^{LS}(\mathbf{r})$ at $t = 1.5 \times 10^{-22}$ s and 6×10^{-22} s are shown in Fig. 6. There is a contact at a certain time between 3.0×10^{-22} s and 4.5×10^{-22} s. Note that the time evolution of density is similar to Fig. 1. The isoscalar dipole mode shown in Fig. 5 suggests that the full overlap is achieved at $t = 5.5 \times 10^{-22}$ s, and the maximal elongation of the composite nucleus at $t = 7.25 \times 10^{-22}$ s. The relaxation of the spin-current tensor contribution is not strongly correlated with that of the isoscalar dipole oscillation (density oscillation toward the fused system). The spin-current tensor contribution is quite small before the contact time (4.2×10^{-22} s), increases after the contact time, achieves local-maximum at $t = 6.75 \times 10^{-22}$ s and 9.00×10^{-22} s, and relaxes afterwards. As is shown in Fig. 6, the difference between the two different frames are negligibly small (see error bars in Fig. 5). Therefore the contribution from the spurious excitation to the spin-current tensor contribution is not important in this case.

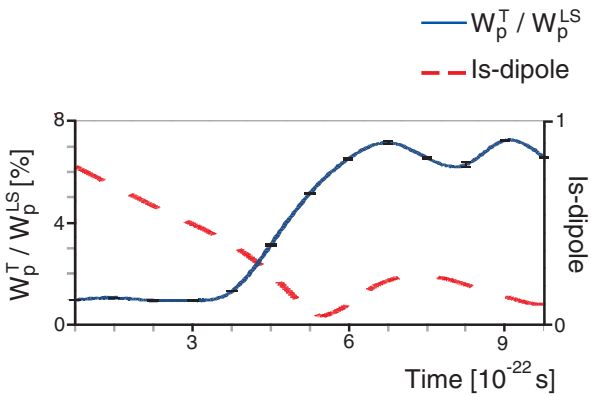

FIG. 5. (Color online) Time evolution of the ratio of contributions from the spin-current tensor terms to those of the spin-orbit terms is shown for protons, where the contribution from the spurious excitation is shown as error bars at some selected points (at multiples of 0.75×10^{-22} s). For reference, the time evolution of the isoscalar dipole (is-dipole) mode in the center-of-mass frame is shown by a dashed line, where the value is normalized by the initial value.

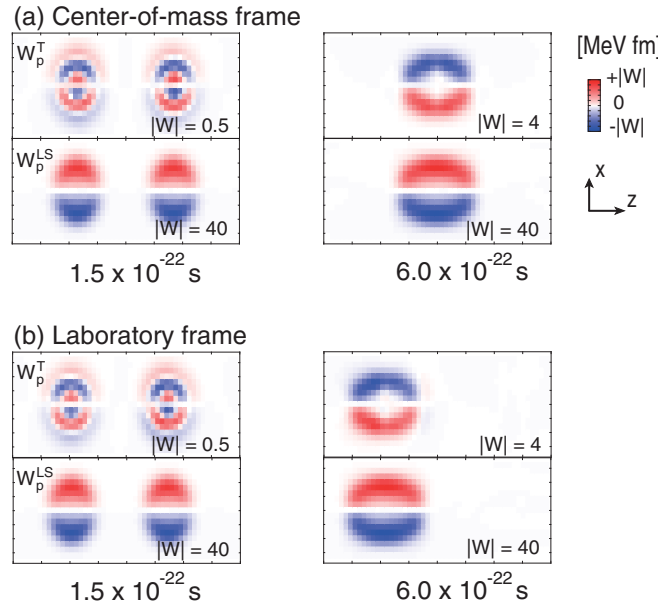

FIG. 6. (Color online) Comparison between calculations in the center-of-mass (a) and laboratory frames (b). Snapshots of the x components of $\mathbf{W}_p^T(\mathbf{r})$ and $\mathbf{W}_p^{LS}(\mathbf{r})$ are shown in a fixed square (40×15 fm^2) for the center-of-mass and laboratory frames. The maximum amplitude $|W|$ of the function is shown in the lower right-hand side of each plot. These situations exactly correspond to the time evolution shown in Fig. 5.

The enhancement of the spin-current tensor contribution is calculated by the ratio

$$S_q = \left| \frac{\mathbf{W}_q^T/\mathbf{W}_q^{LS}(t = 6.5 \times 10^{-22} s)}{\mathbf{W}_q^T/\mathbf{W}_q^{LS}(t = 1.5 \times 10^{-22} s)} \right|, \qquad (7)$$

where $\mathbf{W}_q^T/\mathbf{W}_q^{LS}(t)$ is calculated as shown in Eq. (6). Table IV shows that the enhancement appears independent of the choice of force parameter sets, the effect of spurious excitation is negligibly small, and no significant difference exists between protons and neutrons.

Several points should be remarked here. First, the spin-current tensor contribution is enhanced in collision situations, being up to 10 times larger than before the contact time. Second, the smallness of the spin-current tensor compared to the spin-orbit contributions is noticed. Third, the contribution from the spin-current tensor terms is opposite to the spin-orbit terms if $\alpha + \beta$ is positive, and vice versa. This feature is

TABLE IV. Enhancement of the spin-current tensor contribution for ^{40}Ca + ^{40}Ca. Values of Eq. (7) are calculated for different force parameter sets and isospins. The expectation values for spurious excitation are shown as errors.

Parameter set	S_p	S_n
SV-tls ($\eta_{\rm tls} = 1.0$)	6.62 ± 0.002	6.78 ± 0.009
SLy5+T	9.31 ± 0.061	9.15 ± 0.073
SkM*+Stancu	5.49 ± 0.393	5.54 ± 0.386
SLy4d+Stancu	6.67 ± 0.214	6.71 ± 0.218

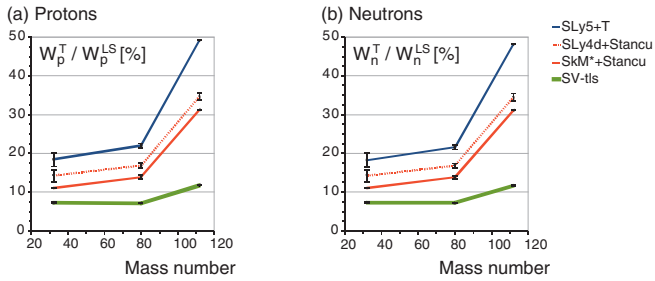

FIG. 7. (Color online) The ratios between spin-current tensor and spin-orbit contributions for protons (a) and neutrons (b) as functions of the mass of the composite nucleus. Calculations with four different force parameter sets are shown, where the maximum values during the initial time evolution until $t = 10 \times 10^{-22}$ s are shown.

apparent during the heavy-ion collision but not before contact. The opposite sign means that the contribution of the tensor force continues to weaken the spin polarization during the reaction. Forth, the similarity between protons and neutrons is confirmed throughout the reaction.

C. Mass dependence

The smallness of the spin-current tensor compared to the spin-orbit contributions is valid independent of the mass, where both $\mathbf{W}_q^T/\mathbf{W}_q^{LS}(t)$ and S_q are larger for heavier systems. Note that the calculations using several different parameter sets result in the same conclusion, hinting that this is probably not strongly force dependent. Moreover, the oppositeness and coincidence in the form factors $\mathbf{W}_q^T$ and $\mathbf{W}_q^{LS}(t)$, which is seen in Fig. 4, is also valid independent of the mass.

Figure 7 shows the mass dependence of the maximum values of the ratio of spin-current tensor compared to spin-orbit contributions reached during the initial time evolution until $t = 10 \times 10^{-22}$ s. In all cases, the times giving the maximal contribution correspond to the time briefly after the first full overlap. For all force parameter sets the same trend appears: the spin-current tensor contribution becomes larger for reactions involving a heavier nucleus. For the heavier cases the contribution from the spin-current tensor terms is almost 50% of that of all spin-orbit terms for SLy5+T. This is not a negligible effect considering the remarkable spin-orbit splitting in the ground states of heavy nuclei, and have a certain impact on superheavy synthesis, since it may affect the dissipation strongly. As the spin-orbit contribution is concentrated on the nuclear surface, such a mass dependence seems to be reasonable.

IV. CONCLUSION

Based on time-dependent density functional calculations with explicitly implemented spin-current tensor terms, the spin-current tensor contribution has been studied in the context of collision dynamics. It is remarkable that the spin-current tensor contribution is enhanced in collision situations. Its contribution is mass dependent so that considerable influence is expected on reactions involving a heavier nucleus. The enhancement and the mass dependence of the spin-current tensor contribution are universal features valid in any heavy-ion reactions independent of additional shell effects possibly occurring in exotic nuclei, which was not a focus of this paper.

Concerning heavy-ion reactions between $N = Z$ identical nuclei, the smallness of the spin-current tensor compared to the spin-orbit contributions has been confirmed independent of mass. Roughly speaking, the amplitude of the spin-current tensor contribution has been clarified to be dependent on the value of $|\alpha + \beta|$, and its sign on the sign of $(\alpha + \beta)$. In particular, the large dissipation due to the spin-orbit force is reduced by the spin-current tensor contribution (the tensor force) for positive $\alpha + \beta$, and enhanced for negative $\alpha + \beta$. We conclude that the spin-current tensor and the tensor-force contribution is rather important in heavy-ion reactions with respect to the magnitude of dissipation. The results presented in this paper give a solid starting point for future research clarifying the role of the tensor force in heavy-ion reactions involving exotic nuclei, where the drastically different contributions from $\mathbf{J}_q$ and $\mathbf{J}_{q'}$ in Eq. (3) might play a significant role.

ACKNOWLEDGMENTS

This work was supported by the Helmholtz Alliance HA216/EMMI and by the German BMBF under Contract No. 06FY9086. The authors would like to thank Profs. P.-G. Reinhard, M. Bender, and N. Itagaki for valuable suggestions.

[1] T. Otsuka, T. Suzuki, R. Fujimoto, H. Grawe, and Y. Akaishi, Phys. Rev. Lett. **95**, 232502 (2005).
[2] T. Otsuka, T. Matsuo, and D. Abe, Phys. Rev. Lett. **97**, 162501 (2006).
[3] T. Otsuka, T. Suzuki, M. Honma, Y. Utsuno, N. Tsunoda, K. Tsukiyama, and M. H.-Jensen, Phys. Rev. Lett. **104**, 012501 (2010).
[4] T. Nakamura *et al.*, Phys. Rev. Lett. **103**, 262501 (2009).
[5] B. A. Brown, T. Duguet, T. Otsuka, D. Abe, and T. Suzuki, Phys. Rev. C **74**, 061303(R) (2006).
[6] T. Lesinski, M. Bender, K. Bennaceur, T. Duguet, and J. Meyer, Phys. Rev. C **76**, 014312 (2007).
[7] G. Colo, H. Sagawa, S. Fracasso, and P. F. Bortignon, Phys. Lett. B **646**, 227 (2007).
[8] M. Bender, K. Bennaceur, T. Duguet, P.-H. Heenen, T. Lesinski, and J. Meyer, Phys. Rev. C **80**, 064302 (2009).
[9] W. Greiner and J. A. Maruhn, *Nuclear Models* (Springer, Berlin, 1996).
[10] J. A. Maruhn, P.-G. Reinhard, P. D. Stevenson, and M. R. Strayer, Phys. Rev. C **74**, 027601 (2006).
[11] D. Vautherin and D. M. Brink, Phys. Rev. C **5**, 3626 (1972).
[12] Fl. Stancu, D. M. Brink, and H. Flocard, Phys. Lett. B **68**, 108 (1977).
[13] A. S. Umar and V. E. Oberacker, Phys. Rev. C **73**, 054607 (2006).
[14] E. Chabanat, P. Bonche, P. Hansel, J. Meyer, and R. Schaeffer, Nucl. Phys. A **635**, 231 (1998); **643**, 441(E) (1998).

[15] K. -H. Kim, T. Otsuka, and P. Bonche, J. Phys. G **23**, 1267 (1997).
[16] J. Bartel, P. Quentin, M. Brack, C. Guet, and H. B. Hakansson, Nucl. Phys. A **386**, 79 (1982).
[17] M. Beiner, H. Flocard, Nguyen Van Giai, and P. Quentin, Nucl. Phys. A **238**, 29 (1975).
[18] P. Ring and P. Schuck, *The Nuclear Many-Body Problem*, 3rd ed. (Springer, Berlin, 2005).
[19] E. B. Suckling and P. D. Stevenson, Eur. Phys. Lett. **90**, 12001 (2010).
[20] S. Fracasso, E. B. Suckling, and P. D. Stevenson, to be submitted.
[21] E. Perlinska, S. G. Rohozinski, J. Dobaczewski, and W. Nazarewicz, Phys. Rev. C **69**, 014316 (2004).
[22] P. Klüpfel, P.-G. Reinhard, T. J. Bürvenich, and J. A. Maruhn, Phys. Rev. C **79**, 034310 (2009).
[23] D. W. L. Sprung, Nucl. Phys. A **182**, 97 (1972).